Posted on 28 Dec 2022 | The copyright holder is the author/funder. All rights reserved. No reuse without permission. | https://doi.org/10.22541/au.167226828.88800119/v1 | This a preprint and has not been peer reviewed. Data may be preliminary.

2,3/1,10-seco, 3-nor guaianolide-type sesquiterpenoids and their derivatives with hypoglycemic activity from *Achillea alpina*

Gui-Min Xue[1], Chen-Guang Zhao[1], Jin-Feng Xue[1], Jiang-Jing Duan[1], Hao Pan[1], Xuan Zhao [1], Zhi-Kang Yang[1], Hui Chen[1], Yan-Jun Sun[1], and Wei-Sheng Feng[1]

[1]Henan University of Chinese Medicine

December 28, 2022

Abstract

Eleven new seco-guaianolide sesquiterpenoids (**1**–**11**) and two new guaianolide dimers (**12** and **13**), along with five known guaianolide derivatives were isolated from the aerial part of *Achillea alpina* L. Compounds **1**–**3** represented three unique 2,3-oxygen inserted guaianolides and **4**–**8** were five special 3-nor guaianolide sesquiterpenoids. Compounds 9–11 were three novel 1,10-seco-guaianolides, while 12 and 13 were two novel 1,10-seco-guaianolides involved heterodimeric [4 + 2] adducts. The new structures of 1–13 including their absolute configurations were determined by spectroscopic data analysis, combined with quantum electronic circular dichroism (ECD) calculations. To evaluate the hypoglycemic activity of **1**–**18**, glucose consumption was used to investigate in palmitic acid (PA)-mediated HepG2-insulin resistance (IR) cells, and compound 9 displayed the strongest reversal IR activity. A mechanistic study has revealed that the potential compound 9 appeared to be mediated hypoglycemic activity via inhibition of the ROS/TXNIP/NLRP3/caspase-1 pathway.

Cite this paper:*Chin. J. Chem.* **2022** , *40* , XXX—XXX. **DOI: 10.1002/cjoc.202200XXX**

2,3/1,10-seco, 3-nor guaianolide-type sesquiterpenoids and their derivatives with hypoglycemic activity from *Achillea alpina*

Gui-Min Xue,* Chen-Guang Zhao, Jin-Feng Xue, Jiang-Jing Duan, Hao Pan, Xuan Zhao, Zhi-Kang Yang, Hui Chen, Yan-Jun Sun, and Wei-Sheng Feng*

College of Pharmacy, Henan University of Chinese Medicine, Zhengzhou 450046, China

Comprehensive Summary

Eleven new seco-guaianolide sesquiterpenoids (**1**–**11**) and two new guaianolide dimers (**12** and **13**), along with five known g

Keywords

Achillea alpina | seco-guaianolide | structure elucidation | hypoglycemic activity | glucose consumption

Background and Originality Content

Sesquiterpenes, formed by three isoprene units with 15 carbons, possess various types of carbon skeletons, such as cadinane-type, eudesmane-type, guaiane-type, calamenene-type and drimane-type.[1] These

Posted on 28 Dec 2022 — The copyright holder is the author/funder. All rights reserved. No reuse without permission. — https://doi.org/10.22541/au.167226828.88800119/v1 — This a preprint and has not been peer reviewed. Data may be preliminary.

secondary metabolites with more than hundreds of carbon skeletons were biosynthetically derived from the mevalonic acid pathway.[2]Sesquiterpenoids possess extensive biological activities, including anti-tumor, anti-inflammatory, antiviral, antifungal and antimicrobial activities, and have been a rich source of bio-active compounds for drug discovery and development.[3] Among them, guaianolide is one of the most representative classes of sesquiterpenoids, and commonly possesses a 5/7/5 tricyclic system, which was widely distributed in the plant family of Composite.[4]

Achillea alpina , belonging to the genus *Achillea*(Composite), is one of eleven species distributed in China, and the aerial part of *A. alpina* was traditionally used as ridding of dampness and detoxification, promoting blood circulation and relieving pain.[5,6] However, the chemical and biological properties of *A. alpina* in China have seldom been investigated until now. Previous researches on *A. alpina* revealed relatively few pharmacological properties, such as antioxidant, hepatoprotective effects and cardiovascular protective activities. Up to date, several types of compounds including flavonoids, sesquiterpenoids, organic acids, triterpenoids have been reported from *A. alpina.* [7,8] Recently, we have also reported some normal germacranolide- and guaianolide-type sesquiterpenoids from the plant.[9] Continuing our effort to explore the structurally interesting and bioactive components from *A. alpina* , eighteen *seco* -guaianolide sesquiterpenoids and their derivatives were isolated. To our best knowledge, compounds **1** –**3**are three rare 2,3-oxygen insertion guaianolides with a 6/7/5 tricyclic rings; **4** –**8** were five unusual 3-*nor* guaianolide sesquiterpenoids with 14 carbons; **9** –**13** were three novel 1,10-*seco* -guaianolides and their dimers (Figure 1). Herein, we describe the isolation, structural elucidation and biological activities of these compounds.

Hosted file

`image3.emf` available at https://authorea.com/users/570207/articles/615934-2-3-1-10-seco-3-nor-guaianolide-type-sesquiterpenoids-and-their-derivatives-with-hypoglycemic-activity-from-achillea-alpina

Figure 1 Chemical structures of compounds**1** –**18 .**

Results and Discussion

Achisecogunolide A (**1**), a white powder, afforded a molecular formula of $C_{20}H_{26}O_7$ on the basis of the (+)-HRESIMS ion peak at *m/z* 401.1580 $[M + Na]^+$ (calcd for 401.1571), corresponding to eight degrees of hydrogen deficiency. The IR spectrum exhibited characteristic absorption bonds for hydroxy (3390 cm^{-1}) and ester carbonyl (1772 and 1703 cm^{-1}) groups. The ^1H NMR spectrum revealed typical signals of three methyl groups (δ_H 1.27, d, J = 7.5 Hz, 3H; 1.62, s, 3H; 1.89, s, 3H), a pair of oxygenated methylene protons (δ_H 4.24, t, J = 17.5 Hz; 4.33, d,J = 17.5 Hz), three oxygenated methines (4.83, d, J = 11.5 Hz; 5.24, ddd, J = 10.5, 5.5, 1.0 Hz; 5.56, s), and an angeloyloxy group (δ_H 1.90, m, 3H; 2.04, dq, J =7.3, 1.5 Hz, 3H; 6.18, qq, J =7.3, 1.5 Hz, 1H) (Table S1).[10] Apart from the angeloyloxy group (δ_C 166.2, 141.2, 126.7, 15.9, 20.5), the^{13}C NMR and HSQC data displayed 15 carbon resonances attributed to three sp^2 carbons (one lactone carbonylδ_C 177.2 and two olefinic carbonsδ_C 141.2, 126.7) and twelve sp^3carbons (including a dioxygenated carbon δ_C 102.2 and five oxygenated carbons δ_C 64.4, 70.2, 75.2, 71.9, 82.2). These NMR signals and MS data suggested **1** to be a sesquiterpene lactone with an angeloyloxy substitution.[11]

Posted on 28 Dec 2022 — The copyright holder is the author/funder. All rights reserved. No reuse without permission. — https://doi.org/10.22541/au.167226828.88800119/v1 — This a preprint and has not been peer reviewed. Data may be preliminary.

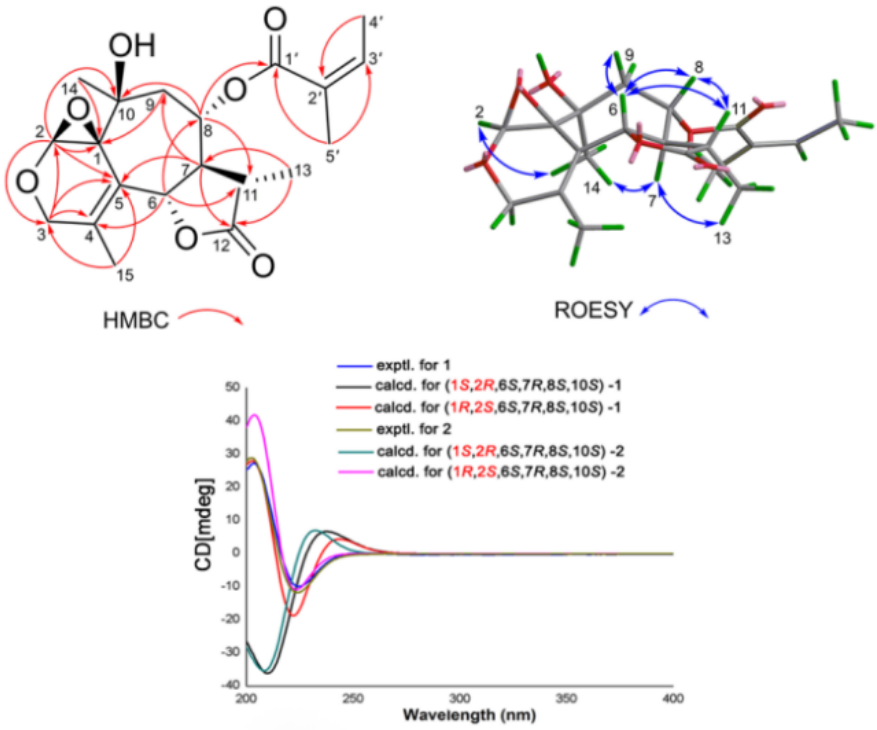

Figure 2 Key HMBC and ROESY correlations of **1** , and experimental and calculated ECD spectra of compounds **1** and **2** .

In the HMBC spectrum, the correlations of H-13 with C-7, C-11 and C-12; H-6 H-7 with C-11 and C-12, confirmed the presence of anα -methyl-γ -lactone moiety. Moreover, the HMBC correlations of H-15/C-3, C-4 and C-5; H-14/C-1, C-9, and C-10; H-6/C-1, C-4, and C-8; H-8/C-6, C-9 and C-11; and H-9/C-1 and C-7 established **1** as a guaiane-type sesquiterpenoid. The locations of angeloyloxy group at C-8 (δ_C 71.9) was deduced from the O -bearing carbon signal at C-8 (δ_C 71.9), and further verified by the HMBC correlation of a deshielded proton H-8 (δ_H 5.24, ddd, J = 10.5, 5.5, 1.0 Hz) with C-1' (δ_C 166.2) (Figure 2). The HMBC correlations of CH_3-15 with olefinic carbons C-4 (δ_C 142.8) and C-5 (δ_C120.9) suggested the presence of the double bond to be located at $\Delta^{4,5}$. An observed chemical shift (δ_C 82.8), together with HMBC corrections of H-14, H-5, and H-8 with C-10, suggested the tertiary hydroxy group to be located at C-10. The HMBC correlations of H-2 (δ_H5.56, s) with the O -bearing carbon C-3 (δ_H64.6), H_2-3 (δ_H 4.23, d, J= 17.5 Hz; 4.32, d, J = 17.5 Hz) with the dioxygenated carbon C-2 (δ_C 102.3) suggested an oxygen atom to be inserted between C-2 and C-3. At this point, the molecule required one epoxy ring to satisfy the remaining one degree of unsaturation. The typical downfield-shifted resonances at C-1 (δ_C72.1) and dioxygenated carbon C-2 (δ_C 102.3) suggested the presence of a 1,2-epoxy group. These were also supported by the observed HMBC correlations of H-14/C-1; H-2/C-1. Thus, the planar structure of **1** was established with a unique C-6/C7/C-5 ring system.

The relative configuration of **1** was speculated from its ROESY spectrum and J -based configurational analysis. On the basis of the large $J_{6,7}$ (11.5 Hz) coupling constant, the orientations of H-6 and H-7 should be opposite,[12] and H-6 and H-7 were assigned asα - andβ -orientation, respectively. The observable ROESY correlations of H-6/H-8, H-9a, and H-11; H-8/H-11 indicated that these protons had the same spatial orientation and were all β -oriented. H_3-14 was defined as α -orientation owing to the ROESY correlation of H-7/H-14 (Figure 2). However, the relative configuration of 1,2- epoxy moiety was difficult to establish with ROESY correlations owing to the distance between H-2 and H-14 were quite close in the 3D structure simulations of **1** for both 1α ,2α or 1β ,2β- epoxy configurations. Thus, the ECD quantum

Posted on 28 Dec 2022 — The copyright holder is the author/funder. All rights reserved. No reuse without permission. — https://doi.org/10.22541/au.167226828.88800119/v1 — This a preprint and has not been peer reviewed. Data may be preliminary.

chemical calculation using the TD-DFT method at the B3LYP/6-311+G(d, 2p) level in the Gaussian 09 program package was used to further confirm its configuration. As shown in Figure 2, the similarity of the experimental spectrum and the calculated ECD with 1β ,2β- epoxy moiety of **1** indicated its 1R ,2S ,6S ,7R ,8S ,10S ,11Sconfigurations. Finally, the structure of **1** was elucidated as shown in Figure 2.

Achisecogunolide B (**2**) displayed a molecular formula of $C_{17}H_{22}O_7$ as deduced from the ^{13}C NMR data (Table S1) and the sodium adduct ion at m/z 361.1261 $[M + Na]^+$ (calcd for 361.1258) in the (+)-HRESIMS. Analysis of the 1D and 2D NMR data of**2** indicated the close similarity of its structure with that of**1** , and the only difference was the replacement of the angeloyloxy moiety at C-8 in **1** by an acetyl group (δ_H 2.10, s; δ_C 21.1, 170.0) in **2** . This was supported by the HMBC correlation from H-8 (δ_H 5.12, ddd, J = 10.5, 5.5, 1.5 Hz) to C-1' (δ_C 170.0), H-2' (δ_H 2.10) to C-1'. The relative configuration of**2** was allocated as identical to that of **1** on the basis of the ROESY spectrum. As shown in Figure 2, the 1R ,2S ,6S ,7R ,8S ,10S ,11Sconfigurations for **2** was established from the similarities of the experimental and the calculated ECD curves.

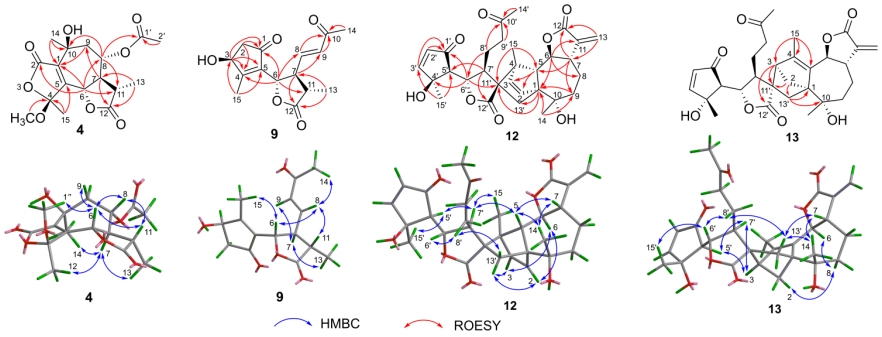

Achisecogunolide C (**3**) possessed a molecular formula of $C_{20}H_{28}O_8$ on the basis of the sodium adduct ion at m/z 419.1669 $[M + Na]^+$ (calcd for $C_{20}H_{28}O_8Na$, 419.1676), suggesting seven degrees of hydrogen deficiency, with less one than that of **1** . The ^1H and ^{13}C NMR data of **3** (Table S1) displayed characteristic signals for a guaianolide sesquiterpenoid, which quite resembled with those of**1** and **2** . A careful comparison of their HRESIMS and NMR data suggested the presence of two hydroxy groups at C-1 and C-2 in**3** , instead of the epoxy moiety in **1** . In the ROESY spectrum, the correlations of H-6/10-OH (δ_H 3.23, s), 10-OH/1-OH (δ_H 2.70, s) suggested the 1-OH to be β -oriented, while 2-OH was α -side supporting by the obvious ROESY correlation of 1-OH with H-2 (δ_H5.06, s) (Figure 3). The absolute configuration of **3** was determined as 1R ,2S ,6S ,7R ,8S ,10S ,11Saccording to the calculated ECD result (Figure 3).

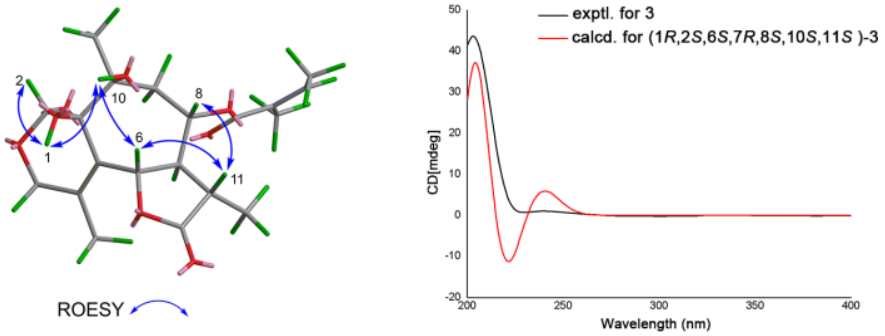

Figure 3 Key ROESY correlations, and experimental and calculated ECD spectra of compound **3** .

Achisecogunolide D (**4**) was assigned the molecular formula $C_{17}H_{22}O_8$ from the positive HRESIMS ion peak at m/z 377.1212 $[M + Na]^+$, corresponding to 7 degrees of hydrogen deficiency. The ^1H NMR spectrum of

Posted on 28 Dec 2022 — The copyright holder is the author/funder. All rights reserved. No reuse without permission. — https://doi.org/10.22541/au.167226828.88800119/v1 — This a preprint and has not been peer reviewed. Data may be preliminary.

4exhibited typical signals for a methoxy group δ_H3.35 (s), three methyl groups (δ_H 1.29, d,J = 7.0 Hz, 3H; 1.66, s, 3H; 1.81, s, 3H), two oxymethine protons (δ_H 5.09, d, J = 11.0 Hz; 5.24, ddd,J = 9.5, 5.5, 3.0 Hz), and an acetyl group (δ_H 2.12, s) (Table S1). Besides the carbon signals for a methoxyl and an acetyl groups, its ^{13}C NMR data supported by the HSQC spectrum revealed that it possessed 14 carbon resonances, which were ascribed to four sp^2carbons (two lactone carbonyl and two olefinic carbons) and twelve sp^3 carbons (including four oxygen-bearing carbons). These characteristic signals, in combination with the MS data, suggested that the carbon skeleton of **4** should be a C_{14}*nor* -sesquiterpenoid.

In the HMBC spectrum of **4** , correlations of H-13 with C-7, C-11 and C-12, and H-6 with C-11, and H-7 with C-11, C-12, and C-13, verified the presence of an α -methylene-γ -lactone moiety (Figure 4). Subsequently, the HMBC correlations of H-6/C-1, C-5, and C-8, H-7/C-5, and C-9, H-8/C-6, C-10, H-14/C-1, C-9, and C-10 (Figure 4) suggested the seven member-ring focused withα -methylene-γ -lactone similar with many other guaianolide sesquiterpenoids. The acetyl and hydroxy groups were respectively attached to C-8 and C-10, according to the key HMBC correlations from H-8 to C-1' (δ_C 169.9), CH_3-14 to C-10 (δ_C 69.9). The HMBC correlations of H-14 with olefinic carbon C-1 (δ_C 135.2), H-15 with olefinic carbon C-5 (δ_C 155.5), and H-6 with C-5 indicated the double bond to be located at $\Delta^{1,5}$(Figure 4). Furthermore, the HMBC cross peak of CH_3-15 and OCH_3-1" with the downfield chemical shift atδ_C 108.6 suggested C-4 to be a two oxygen-bearing carbon, and the other connected oxygen to C-4 was deduced to be an extra lactone carbonyl (C-2, δ_C 169.1). This was exactly matched with the remaining unsaturation and molecular formula, and was also demonstrated by long-range HMBC correlation between H-6 and C-2. In the ROESY spectrum, the correlations of H-6/H-8, H-6/H-11, H-6/H-9a, H-6/H-1", H-8/H-11, indicated that H-6, H-8, H-11, and 1"-OCH_3 were allβ -oriented, while H-7, H_3-13, H_3-14, H_3-15 was defined asα -oriented owing to the ROESY correlations of H-7/H_3-13, H_3-14, H_3-15 (Figure 4). The absolute configuration for **4** was established as 4S ,6S ,7R ,8S ,10S ,11S through calculated ECD method (Figure 5).

The same molecular formula $C_{17}H_{22}O_8$ of **5**as that of **4** was established on the basis of its HRESIMS ion atm/z 377.1211 $[M + Na]^+$. The resonances in its ^{1}H and ^{13}C NMR, HSQC, and HMBC data indicated that the planar structure of **5** was identical to that of **4** . In the ROESY spectrum (Figure 4), the correlations of H_3-15/H-6, H-7/1"-OCH_3 were indicative of a 4α -OCH_3in **5** , which was opposite to that of **4** . The experimental ECD spectrum of **5** was similar to calculated ECD, suggesting the 4R ,6S ,7R ,8S ,10S ,11Sabsolute configurations of **5** (Figure 5). Hence, the structure of **5** was established as shown, and named achisecogunolide E.

The (+)-HRESIMS and ^{13}C NMR data of achisecogunolide F (**6**) was indicative of a molecular formula of $C_{16}H_{20}O_8$, with 14 mass units less than that of **5** . Comparing the NMR data of **6**with those of **5** revealed many similarities, except for the replacement of the methoxy group at C-4 in **5** by a hydroxyl group in **6** . The hydroxyl group was defined asβ -orientation owing to the ROESY correlations of H_3-15 and H-7. According to the application of TD-DFT ECD calculation method, the similarity of calculated ECD spectrum with its experimental one suggested the 4S ,6S ,7R ,8S ,10S ,11Sconfigurations of **6** (Figure 5).

Achisecogunolide G (**7**) displayed a molecular formula of $C_{20}H_{26}O_8$ as assigned from the sodium adduct ion at m/z 417.1529 (calcd for 417.1520) in the (+)-HRESIMS. Its 1D and 2D NMR spectra revealed that it is structurally similar to that of **4** . The only difference was the presence of an angeloyloxy moiety (δ_H 1.90, m, 3H; 2.06, dq, J =7.5, 1.5 Hz, 3H; 6.22, qq, J =7.5, 1.5 Hz, 1H) in **7** instead of the acetyl group in **4** . The 8-O -angeloyl group was defined by the HMBC correlation from H-8 (δ_H 5.53, ddd, J = 9.5, 5.0, 3.0) to the carbonyl of the angeloyl group. The 4-OCH_3 was also deduced as β -oriented due to the ROESY correlations of 4-OCH_3 /H-6. The absolute configuration of **7**was established as 14S ,6S ,7R ,8S ,10S ,11S by using similar ECD calculation (Figure 5).

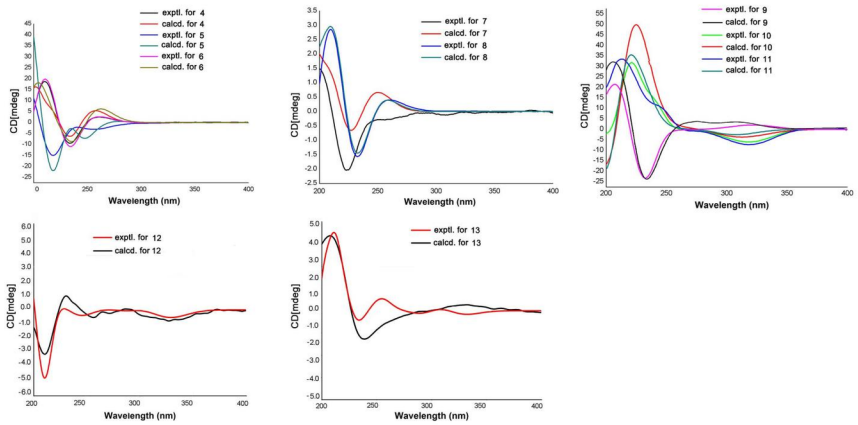

Achisecogunolide H (**8**) gave a molecular formula of $C_{19}H_{24}O_8$ as deduced from the ^{13}C NMR data (Table S2) and the sodium adduct (+)-HRESIMS ion at *m/z* 381.1531 $[M + H]^+$. Scrutiny of the NMR data of **8** suggested the close similarity of its structure with that of **7** , and the only difference was the replacement of the methoxy group in **7** by a hydroxy unit at C-4 in **8** as supported by the shielded C-4 (δ_C 104.4). The above assignment was supported by the analysis of the HMBC spectrum. The relative configuration of**8** was identical to **7** following the analysis of the ROESY spectrum. The absolute configuration of **8** was defined as 4*S* ,6*S* ,7*R* ,8*S* ,10*S* ,11*S* via calculated ECD result (Figure 5).

Achisecogunolides I and J (**9** and **10**) possessed the same molecular formula $C_{15}H_{18}O_5$ on the basis of HRESIMS peaks at *m/z* 301.1074 $[M + Na]^+$(calcd for 301.1046) and 279.1234 $[M + H]^+$ (calcd for 279.1227), respectively. The 1D NMR data of **9** were comparable to those of **10** , indicating that they were quite similar structures. The 1D and 2D NMR data analysis suggested that they were similar to those of *iso* -*seco* -tanapartholide, a guaianolide sesquiterpenoid with a 1,10-splited ring carbon skeleton.[13] This was supported from the HMBC correlations of H-2 and H-3 with C-1, C-4 and C-5; H-5 with C-1, C-2, C-3 and C-7; H-6 with C-1, C-8 and C-11; H-8, H-9 and H-14 with C-10; H-13 with C-7 and C-12; H-15 with C-3 and C-5. Comparison of the NMR data of **9** and **10** with those of*iso* -*seco* -tanapartholide, the difference was the presence of a *trans* -double bond signals at δ_H 6.62 (dd, J = 16.0, 8.5 Hz) and 6.13 (d, J = 16.0 Hz) in**9** , δ_H 6.61 (dd, J = 16.0, 8.5 Hz) and 6.11 (d, J = 16.0 Hz) in **10** , and the double bond was located between C-8 and C-9 owning to HMBC correlations of H-8, H-9 with C-10 and C-7, H-7 with C-8 and C-9. Thus, the planar structures of**9** and **10** were established, and their structural differences were in stereoscopic configuration. In their ROESY spectra, the identical correlations of H-6/H-11, H-7/-13 was observed (Figure 4). Thus, the difference was presence at the chiral center C-3. The configurations of C-3 in **9** and **10** were further defined by ECD quantum chemical calculation. As shown in Figure 5, the 3*S*configuration for **9** and 3*R* configuration for **10**was determined from the similarities of the experimental and the calculated ECD curves (Figure 5). Eventually, the structures of**9** and **10** were elucidated and named achisecogunolides I and J, respectively.

Achisecogunolide K (**11**) had a molecular formula of $C_{16}H_{20}O_5$ according to HRESIMS at *m/z* 293.1392 [M + H]$^+$ (calcd for 293.1384) with a difference of 15 Da more than that of compound**11** . Analysis of the NMR spectroscopic data suggested that**11** shared the same 1,10-splited guaianolide-type sesquiterpene skeleton as that of **10** , except that the hydroxyl group substituent at C-3 was replaced by a methoxy group (δ_H 3.42, s), as corroborated by HMBC correlations from 1'-OCH_3 to C-3. The calculated ECD data facilitated the determination of the 3*S* ,6*R* ,7*S* ,11*S* absolute configuration of**11** .

Posted on 28 Dec 2022 — The copyright holder is the author/funder. All rights reserved. No reuse without permission. — https://doi.org/10.22541/au.167226828.88800119/v1 — This a preprint and has not been peer reviewed. Data may be preliminary.

Posted on 28 Dec 2022 — The copyright holder is the author/funder. All rights reserved. No reuse without permission. — https://doi.org/10.22541/au.167226828.88800119/v1 — This a preprint and has not been peer reviewed. Data may be preliminary.

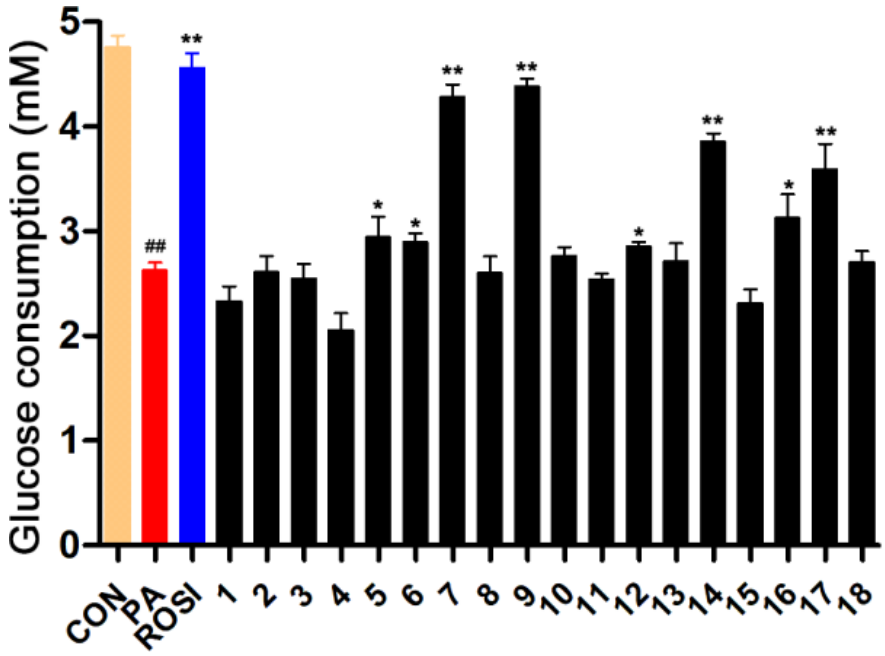

Figure 6 The glucose consumption assay for compounds **1** –**18** (50 μM). ROSI (50 μM) was the positive control. $^{*}p < 0.05$, $^{**}p < 0.01$, compared to PA group.

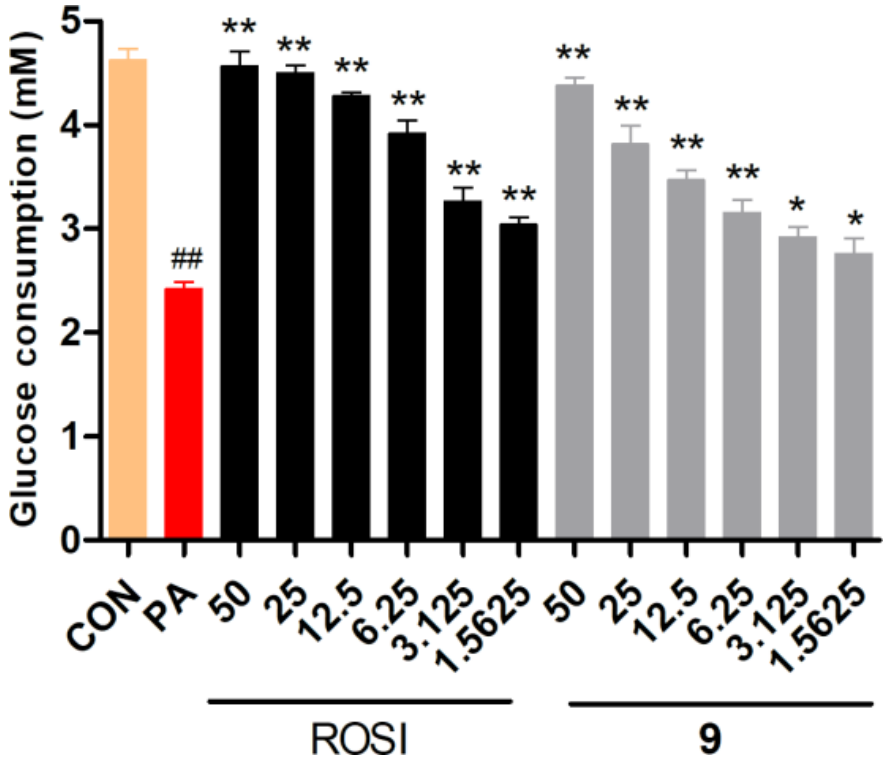

Figure 7 The glucose consumption assay of **9** in different concentrations from 1.5625 to 50 μM. ROSI was the positive control. $^{*}p < 0.05$, $^{**}p < 0.01$, compared to PA group. $^{\#\#}p < 0.01$, compared to CON group.

Posted on 28 Dec 2022 — The copyright holder is the author/funder. All rights reserved. No reuse without permission. — https://doi.org/10.22541/au.167226828.88800119/v1 — This a preprint and has not been peer reviewed. Data may be preliminary.

Achisecogunolide L (**12**) was obtained as a white powder. A sodium adduct ion peak at *m/z* 547.2305 ([M + Na]$^+$, calcd for 547.2302) in HRESIMS suggested its molecular formula to be $C_{30}H_{36}O_8$, corresponding with 13 indices of hydrogen deficiency. The IR spectrum showed absorption bands for hydroxy (3460 cm^{-1}), ester carbonyl (1760 cm^{-1}), and carbonyl (1753, 1702, 1643 cm^{-1}) functionalities. Both the ^{1}H and ^{13}C NMR data of **12** were similar to those of 1,10-*seco* -guaianolide involved heterodimeric [4 + 2] Diels-Alder adduct of **18** , an sesquiterpenoid dimer which were isolated from genus *Achillea* .[14] The structural difference involved the position of a *cis* -double bond by analyses of the NMR data. The HMBC correlations of H-2*'*(δ_H 6.18, d, J = 5.7 Hz), H-3*'*(δ_H 7.46, d, J = 5.7 Hz)/C-1*'*(δ_C 204.7), and C-4*'*(δ_C 78.5), and H_3-15*'* /C-4*'* , assigned the double bond $\Delta^{2'(3')}$. Besides, the presence of the hydroxyl group was located at C-4*'* based on the HMBC correlation between H_3-15*'* and C-4*'* . The linkages of C-1-C-13' and C-4-C-11' between the 1,10-*seco* -guaianolide and guaianolide parts were established the same as that of **18** , based on the HMBC correlations from H-1 to C-11' and C-13'; from H-13' to C-1, C-2, C-4'; from H-15 to C-11'. The ROESY correlations of H-2/H-6, H-3/H-6 (Figure 4) demonstrated the 2*α* ,3*α* -ethylidene bridge in the formative five-membered ring C-1–C-13'–C-11'–C-4–C-5. The presence of 4'-OH was defined asβ -orientation owing to the ROESY correlations of H-5'/H-15', H-5'/H-7'. The absolute configuration of **12** was also deduced from the ECD calculation. As shown in Figure 5, the calculated ECD spectrum of (1*R* ,4R,5*S* ,6*S* ,7*S* ,10*R* ,4*'S* ,5*'S* ,6*'S* ,7*'S* ,11*'R*)**-12**was agreed well with the experimental spectrum, leading to the assignment of the absolute configuration. Thus, the structure of**12** was elucidated as shown, and named achisecogunolide L.

Achisecogunolide M (**13**) afforded the molecular formula $C_{30}H_{36}O_8$ as established by the HRESIMS ion at *m/z* 547.2311 ([M + Na]$^+$, calcd for 547.2302) and^{13}C-NMR data. Analysis of its ^{1}H and^{13}C NMR, HSQC, and HMBC spectra (Table S3) implied that **13** was also a sesquiterpenoid dimer and had a very similar structure as that of **12** . Comparison of the position of a double bond at $\Delta^{2,3}$ in **12** , the presence of double bond in **13** was located at $\Delta^{4,5}$, which was supported by downfield chemical shift alkenylmethyl at H_3-15 (δ_H 2.02, s) and HMBC correlations of H_3-15/C-4, C-5. This suggested that the [4 + 2] Diels-Alder reaction position for the two sesquiterpenoid units was changed. In the HMBC spectrum, the correlations of H_2-13*'* /C-1 and C-10; H-3/C-7*'* , C-11*'* and C-12*'*, H-2/C-11*'* and C-13*'*indicated the connection of two units were through C-1–C-13*'* and C-3–C-11*'*. The ROESY correlations of H-15*'*/ H-6*'* , H-6*'*/ H-8*'* , H-8*'*/ H-13*'* , H-13*'*/ H-7, indicated that those protons were co-facial and assigned asβ -orientation. On the basis of the ROESY correlations of H-5*'* /H-7*'* , H-7*'* /H-3, H-3/H-2, H-2/H-8, H-8/H-6 and the large coupling constants of H-5*'* /H-6*'* (J = 10.0 Hz), H-6*'* /H-7*'* (J = 10.0 Hz), H-6/H-7 (J = 10.2 Hz), suggested that H-5*'*, H-7*'*, H-6, and the bridge of -2-CH_2- were all *α* -oriented. The absolute configuration of **13** was defined as (1*S* ,3*R* ,6*S* ,7*S* ,10*R* ,4*'R* ,5*'S* ,6*'S* ,7*'S* ,11*'S*) by comparison of the experimental and calculated ECD data (Figure 5). Thus, the structure of achisecogunolide M (**13**) was defined, and to our best knowledge, **13** was the first 1,10-*seco*guaianolide involved heterodimeric [4 + 2] Diels-Alder sesquitenpenoid dimer in a C-1–C-13*'* and C-3–C-11*'*linkage mode.

Five known compounds were identified as millefoliumin C (**14**),[15] millefoliumin A (**15**),[15]*iso* -*seco* -tanapartholide (**16**),[16]3*α* -*O* -hydroxyl-*iso* -*seco* -tanapartholide (**17**) [17], achillinin C (**18**)[14] based on their spectroscopic data.

Compounds **1** –**18** were examined with respect to their reversal IR activity in PA-activated HepG2 cells. Cell viability was evaluated by CCK-8 assay, and none of the test compounds showed significant cytotoxicity at their effective concentration (Figure S1). The concentration of PA at 200 μ M was used to establish the HepG2-IR model,[18] and the significantly lower glucose consumption was observed either in the absence or presence of insulin in HepG2 cells[11]. As shown in Figure 6, some 3-*nor* (**7** and **14**) and 1,10-*seco*guaianolide-type sesquiterpenoids (**9** and **17**) showed promising reversal IR activities compared with the positive control ROSI (50.0 μ M).

Posted on 28 Dec 2022 — The copyright holder is the author/funder. All rights reserved. No reuse without permission. — https://doi.org/10.22541/au.167226828.88800119/v1 — This a preprint and has not been peer reviewed. Data may be preliminary.

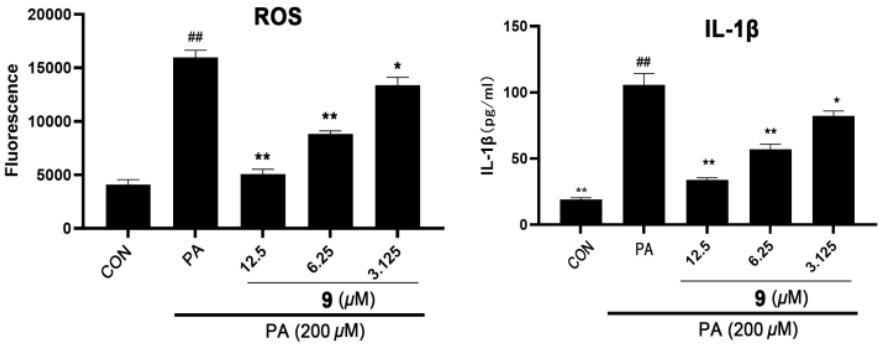

Figure 8 The inhibitory effects of compound **9** on ROS and IL-1β in HepG2-IR cells. $^{*}p < 0.05$, $^{**}p < 0.01$, compared to PA group. ##p < 0.01, compared to CON group.

The most potential compound **9** was further tested for their reversal IR activity at the concentrations from 1.5625–50.0 μ M, and the increased glucose consumption in a dose-dependent manner in PA-treated HepG2 cells was observed (Figure 7). Pharmacological studies have revealed that the excessive secretion of inflammatory factors especially IL-1β and ROS overproduction could promote the development of IR for diabetes,[19] and PA-induced IR of HepG2 cells could lead to the secretion of inflammatory cytokines and trigger the formation of ROS overproduction.[20,21] As shown in Figure 8, PA treatment obviously enhanced the levels of IL-1β related to control group. Expectedly, pretreatment of the **9**dose-dependently suppressed IL-1β expression in ELISA assay. Similarly, the overproduction of ROS in PA-induced HepG2 cells was also inhibited by **9** (Figure 8).

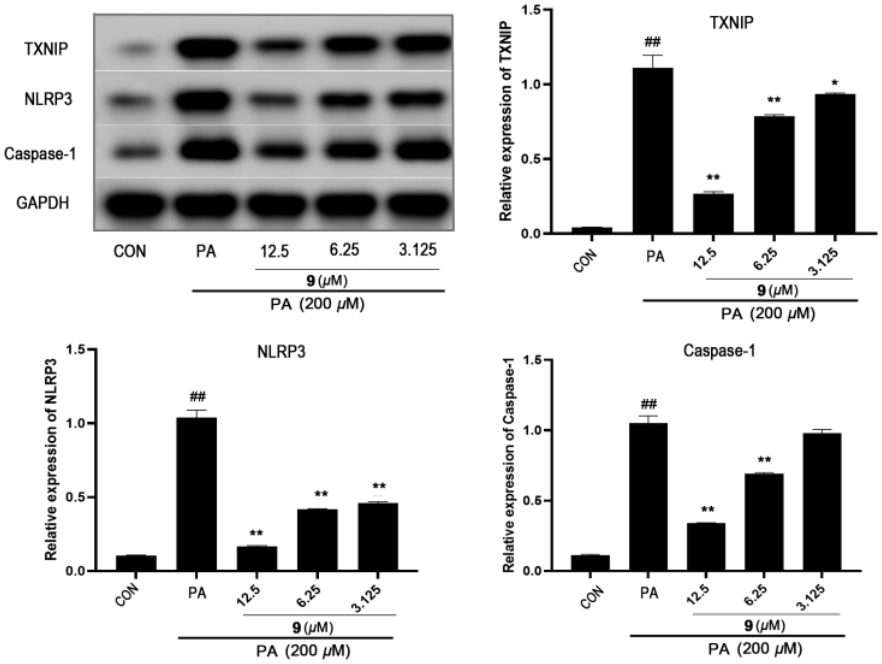

Figure 9 Inhibitory effect of compound **9** on NLRP3 signaling pathway. Western blot analysis with antibodies specific for TXNIP, NLRP3, caspase-1 and GAPDH proteins in PA-induced HepG2 cells. $^{*}p < 0.05$, $^{**}p < 0.01$, compared to PA group. $^{\#\#}p < 0.01$, compared to CON group.

Since the excessive production of IL-1β and ROS in diabetes are closely associated to activation of the NLRP3

Posted on 28 Dec 2022 — The copyright holder is the author/funder. All rights reserved. No reuse without permission. — https://doi.org/10.22541/au.167226828.88800119/v1 — This a preprint and has not been peer reviewed. Data may be preliminary.

inflammasome signal pathway.[22] Thus, the expression levels of proteins related to the signal pathway was detected by Western blotting assay. As shown in Figure 9, the protein levels of TXNIP, NLRP3 and caspase-1 proteins in PA-induced HepG2 cells were increased compared to the control group, while compound **9** significantly suppressed the expressions of TXNIP, NLRP3 and caspase-1 proteins at concentrations of 3.125-12.5 μ M. These results demonstrated that **9**reduced IR of PA-induced HepG2 cells through inhibiting of the NLRP3 inflammasome signaling pathway.

Conclusions

In the present study, chemical investigation on the aerial part of*A. alpina* led to the isolation of eighteen*seco* -guaianolides and their derivatives (**1** –**18**). Among them, compounds **1** –**3**represented three unique 2,3-oxygen inserted guaianolides and**4** –**8** were five special 3-*nor* guaianolide sesquiterpenoids. Compound **13** was the first 1,10-*seco* -guaianolides involved heterodimeric [4 + 2] adduct connection through C-1–C-13*'* and C-3–C-11*'*. The structures were elucidated on the basis of extensive NMR spectroscopic data analyses and calculated ECD method. All compounds were tested for their hypoglycemic activity in PA-induced HepG2-IR cells. The results have revealed that compound **9** promoted the glucose consumption even at the low concentrations of 3.125 μM. Moreover, compound**9** decreased the expression of IL-1β and the generation of ROS, and also down-regulated the protein levels of TXNIP, NLRP3 and caspase-1, suggesting compound **9** mediated IR via suppression of NLRP3 inflammasome pathway. To our best knowledge, sesquiterpenoids with reversal IR activity have rarely been reported. Thus, we believe that they will be of great interest to chemists and pharmacologists for further research on their synthesis, structure modification, and pharmacological mechanisms.

Experimental

General Experimental Procedures

A JASCO 810 spectropolarimeter (JASCO, Tokyo, Japan) was used to measure ECD spectra. Optical rotations were operated on a JASCO P-1020 polarimeter in MeOH, and UV spectra were recorded using a UV-2450 visible spectrophotometer. IR spectra (in MeOH) were measured on a Bruker Tensor 27 spectrometer (Bruker, Karlsruhe, Germany). Nuclear magnetic resonance (NMR) spectra were recorded on Bruker AVIII-500 and -600 spectrometers (Bruker, Karlsruhe, Germany). HRESIMS data were recorded with an Agilent 6520B Q-TOF mass spectrometer (Agilent Technologies, Santa Clara, USA) and an AB Sciex Triple-TOF 6600 (AB SCIEX, Framingham, USA). *Pre* -HPLC was carried out on a Separation LC-120 system (Separation, Beijing, China) using a YMC-pack RP-C_{18} column (250 mm × 20 mm i.d., 5 μ m, YMC, Tokyo, Japan). Column chromatography (CC) were performed on MCI (Mitsubishi, Japan), Sephadex LH-20 (Pharmacia Biotech AB, Uppsala, Sweden) and RP-C_{18} silica (40-63 μ m, FuJi, Japan). Analytical grade of all solvents (JTJshield Fine Chemicals Co., Ltd., Tianjin, China) were used in the separation process.

Plant Material

The aerial part of *A. alpina* was collected in May 2020 from Kunming, Yunnan Province, China, and identified by Dr Lin-Lin Yang (Henan University of Chinese Medicine, ZhengZhou, China). A voucher specimen (No.202005) was deposited at the Discipline of TCM & Chemistry of Natural Products, College of Pharmacy, Henan University of Chinese Medicine.

Extraction and Isolation

The aerial part of *A. alpina* (5.0 kg) was extracted with methylene dichloride (4×10 L) at room temperature. The percolates were combined and evaporated under reduced pressure to give a crude extract (52.0 g). The crude extract was subjected to a MCI CC eluted with aqueous MeOH in a gradient manner (10%, 30%, 60%, 80%, 90% and 100%) yielding six fractions BM1–BM6. The BM3 fraction (8.4 g) was subjected to a Sephadex LH-20 to afford six subfractions (BM3N1–BM3N6).

Subfraction BM3N2 was subjected to RP-C_{18} CC eluted with a step-wise gradient of aqueous MeOH (100:0–0:100) to obtain 18 fractions (BM3N2O1–BM3N2O20). Then, subfraction BM3N2O13 was further purified

Posted on 28 Dec 2022 — The copyright holder is the author/funder. All rights reserved. No reuse without permission. — https://doi.org/10.22541/au.167226828.88800119/v1 — This a preprint and has not been peer reviewed. Data may be preliminary.

with *pre* -HPLC (CH_3CN:H_2O 30:70–70:30, 50 min) to yield compounds **12** (44.0 mg, t_R = 24.2 min) and **18** (3.8 mg, t_R = 26.8 min). BM3N2O14 was conducted on*pre* -HPLC (MeOH:H_2O 60:40) to yield compound**13** (4.1 mg, t_R = 29.1 min).

Subfraction BM3N3 was subjected to RP-C_{18} CC eluted with aqueous MeOH to give 15 fractions (BM3N3O1–BM3N3O15). Subsequently, subfraction BM3N3O12 was further separated with *pre* -HPLC (CH_3CN:H_2O 30:70–70:30, 50 min) to give compound **8** (8.7 mg, t_R = 25.0 min).

Subfraction BM3N4 was subjected to a RP-C_{18} CC (150 g, eluted with 10-100% MeOH/H_2O, v/v) to afford 15 fractions BM3N4O1–BM3N4O15. Fraction BM3N4O3 was further purified with *pre* -HPLC (CH_3CN:H_2O 10:90–40:60, 50 min) to yield compounds **9** (1.8 mg, t_R = 28.2 min) and**10** (1.9 mg, t_R = 30.2 min). Fraction BM3N4O4 was separated by *pre* -HPLC (CH_3CN:H_2O 10:90–40:60, 50 min) to yield compounds **16** (2.4 mg, t_R = 23.9 min) and**17** (2.5 mg, t_R = 33.8 min). Fraction BM3N4O5 was separated by *pre* -HPLC (CH_3CN:H_2O 10:90–50:50, 50 min) to yield compounds **2** (2.1 mg, t_R = 30.1 min),**3** (2.3 mg, t_R = 29.0 min) and **11** (2.1 mg, t_R = 26.8 min). Subfraction BM3N4O8 was purified with *pre* -HPLC (CH_3CN:H_2O 10:90–70:30, 50 min) to yield compounds **4** (2.0 mg, t_R = 24.3 min) and **5** (3.2 mg, t_R = 20.1 min). Subfraction BM3N4O10 was subjected to*pre* -HPLC (CH_3CN:H_2O 30:70–70:30, 50 min) to yield compounds **6** (4.8 mg, t_R = 22.3 min) and **15** (2.8 mg, t_R = 27.8 min). Subfraction BM3N4O11 was purified with *pre* -HPLC (CH_3CN:H_2O 20:80–65:35, 50 min) to yield compound **1** (4.3 mg, t_R = 41.5 min). Subfraction BM3N4O12 was subjected to *pre* -HPLC (CH_3CN:H_2O 35:65–80:20, 50 min) to yield compounds **7** (3.5 mg, t_R = 27.9 min) and**14** (7.9 mg, t_R = 25.8 min).

Achisecogunolide A (**1**): White powder; [α]25 D +53.2 (*c* 0.1, MeOH); UV (MeOH) λ_{max} 212 nm; ECD (MeOH) λ_{max} ($\Delta\epsilon$) 215 (-9.93) 243 (+0.14) nm; IR (KBr) ν_{max}/cm^{-1} 3389, 1772, 1702, 1644,1450, 1380, 1227, 1143, 1120, 1042, 983, 860;^{1}H and ^{13}C NMR data (Table S1); HRESIMS *m/z* 401.1580 [M + Na]$^+$ (calcd for $C_{20}H_{26}O_7Na$, 401.1571).

Achisecogunolide B (**2**): White powder; [α]25 D +42.3 (*c* 0.1, MeOH); UV (MeOH) λ_{max} 224 nm; ECD (MeOH) λ_{max} ($\Delta\epsilon$) 214 (-11.8) nm; IR (KBr)ν_{max}/cm^{-1} 3403, 1767, 1733, 1639, 1450, 1374, 1254, 1145, 1089, 983, 863; ^{1}H and^{13}C NMR data (Table S1); HRESIMS *m/z* 361.1261 [M + Na]$^+$ (calcd for $C_{17}H_{22}O_7Na$, 361.1258).

Achisecogunolide C (**3**): White powder; [α]25 D +43.0 (*c* 0.03, MeOH); UV (MeOH) λ_{max} 218 nm; ECD (MeOH) λ_{max} ($\Delta\epsilon$) 203 (+43.7), 240 (+1.04) nm; IR (KBr) ν_{max}/cm^{-1} 3474, 1759, 1702, 1645, 1456, 1358, 1237, 1160, 1066, 959;^{1}H and ^{13}C NMR data (Table S1); HRESIMS *m/* z 419.1669 [M + Na]$^+$ (calcd for $C_{20}H_{28}O_8Na$, 419.1676).

Achisecogunolide D (**4**): White powder; [α]25 D +58.6 (*c* 0.1, MeOH); UV (MeOH) λ_{max} 210 nm; ECD (MeOH) λ_{max} ($\Delta\epsilon$) 210 (+18.74), 234 (-9.44), 261 (+2.48) nm; IR (KBr)ν_{max}/cm^{-1} 3387, 1761, 1647,1455, 1379, 1246, 1165, 1027; ^{1}H and^{13}C NMR data (Table S1); HRESIMS *m/z* 377.1212 [M + Na]$^+$ (calcd for $C_{17}H_{22}O_8Na$, 377.1207).

Achisecogunolide E (**5**): White powder; [α]25 D +26.9 (*c* 0.1, MeOH); UV (MeOH) λ_{max} 232 nm; ECD (MeOH) λ_{max} ($\Delta\epsilon$) 218 (-15.01), 256 (-3.10) nm; IR (KBr) ν_{max}/cm^{-1} 3406, 1756, 1452, 1385, 1262, 1168, 1101, 1064, 1028, 805;^{1}H and ^{13}C NMR data (Table S1); HRESIMS *m/z* 377.1211 [M + Na]$^+$ (calcd for $C_{17}H_{22}O_8Na$, 377.1207).

Achisecogunolide F (**6**): White powder; [α]25 D +60.4 (*c* 0.2, MeOH); UV (MeOH) λ_{max} 226 nm; ECD (MeOH) λ_{max} ($\Delta\epsilon$) 211 (+19.81), 234 (-11.00), 261 (+2.60) nm; IR (KBr)ν_{max}/cm^{-1} 3372, 1758, 1454, 1380, 1245, 1166, 1028, 914, 802; ^{1}H and^{13}C NMR data (Table S1); HRESIMS *m/z* 363.1054 [M + Na]$^+$ (calcd for $C_{16}H_{20}O_8Na$, 363.1050).

Achisecogunolide G (**7**): White powder; [α]25 D -10.9 (*c* 0.1, MeOH); UV (MeOH) λ_{max} 216 nm; ECD (MeOH) λ_{max} ($\Delta\epsilon$) 210 (+28.56), 233 (-15.65), 260 (+4.01) nm; IR (KBr)ν_{max}/cm^{-1} 3476, 1762, 1710, 1645, 1456, 1379, 1277, 1235, 1154, 1041, 1018, 914, 851;^{1}H and ^{13}C NMR data (Table S2); HRESIMS *m/z* 417.1529 [M + Na]$^+$ (calcd for $C_{20}H_{26}O_8Na$, 417.1520).

Posted on 28 Dec 2022 — The copyright holder is the author/funder. All rights reserved. No reuse without permission. — https://doi.org/10.22541/au.167226828.88800119/v1 — This a preprint and has not been peer reviewed. Data may be preliminary.

Achisecogunolide H (**8**): White powder; [α]25 D -6.3 (c 0.1, MeOH); UV (MeOH) λ_{max} 210 nm; ECD (MeOH) λ_{max} ($\Delta\epsilon$) 200 (+1.50), 223 (-2.04) nm; IR (KBr) ν_{max}/cm^{-1} 3385, 1750, 1644, 1456, 1381, 1237, 1158, 1024; ^{1}H and^{13}C NMR data (Table S2); HRESIMS m/z 381.1531 [M + H]$^+$ (calcd for $C_{19}H_{24}O_8$, 381.1544).

Achisecogunolide I (**9**): White powder; [α]25 D -87.4 (c 0.1, MeOH); UV (MeOH) λ_{max} 224 nm; ECD (MeOH) λ_{max} ($\Delta\epsilon$) 207 (+21.40), 232 (-23.29), 323 (+2.06) nm; IR (KBr)ν_{max}/cm^{-1} 3440, 1774, 1658, 1408, 1261, 1097, 1024, 802; ^{1}H and^{13}C NMR data (Table S2); HRESIMS m/z 301.1074 [M + Na]$^+$ (calcd for $C_{15}H_{18}O_5$Na, 301.1046).

Achisecogunolide J (**10**): White powder; [α]25 D -21.2 (c 0.3, MeOH); UV (MeOH) λ_{max} 210 nm; ECD (MeOH) λ_{max} ($\Delta\epsilon$) 220 (+31.85), 318 (-6.04) nm; IR (KBr) ν_{max}/cm^{-1} 3415, 1768, 1652, 1453, 1383, 1261, 1177, 1106, 1022, 981, 804;^{1}H and ^{13}C NMR data (Table S2); HRESIMS m/z 279.1234 [M + H]$^+$ (calcd for $C_{15}H_{19}O_5$, 279.1227).

Achisecogunolide K (**11**): White powder; [α]25 D -21.8 (c 0.5, MeOH); UV (MeOH) λ_{max} 210 nm; ECD (MeOH) λ_{max} ($\Delta\epsilon$) 213 (+33.50), 319 (-7.29) nm; IR (KBr) ν_{max}/cm^{-1} 3405, 1779, 1708, 1674, 1456, 1383, 1249, 1171, 1099, 1021, 985;^{1}H and ^{13}C NMR data (Table S2); HRESIMS m/z 293.1392 [M + H]$^+$ (calcd for $C_{16}H_{21}O_5$, 293.1384).

Achisecogunolide L (**12**): White powder; [α]25 D -56.6 (c 0.1, MeOH); UV (MeOH) λ_{max} 210 nm; ECD (MeOH) λ_{max} ($\Delta\epsilon$) 209 (-2.28), 234 (+0.54), 259 (-0.34), 330 (-0.70), nm; IR (KBr)ν_{max}/cm^{-1} 3460, 1753, 1702, 1643, 1458, 1386, 1266, 1164, 987; ^{1}H and^{13}C NMR data (Table S3); HRESIMS m/z547.2305 [M + Na]$^+$ (calcd for $C_{30}H_{36}O_8$Na, 547.2302).

Achisecogunolide M (**13**): White powder; [α]25 D +19.2 (c 0.1, MeOH); UV (MeOH) λ_{max} 210 nm; ECD (MeOH) λ_{max} ($\Delta\epsilon$) 208 (+4.21), 239 (-1.59), 332 (+0.33) nm; IR (KBr) ν_{max}/ cm^{-1} 3452, 1755, 1707, 1646, 1455, 1383, 1257, 1147, 1001, 719; ^{1}H and ^{13}C NMR data (Table S3); HRESIMS m/z 547.2311 [M + Na]$^+$(calcd for $C_{30}H_{36}O_8$Na, 547.2302).

ECD Calculations

The relative configurations of **1** –**13** were established initially according to their ROESY NMR spectra. All conformational searches used the MMFF94s force field. Conformers having internal relative energies within 3 kcal/mol were subjected to geometry optimization by the density functional theory (DFT) method at the B3LYP/6-31G(d,p) level in Gaussian 09 program package. These optimized conformers were then subjected to TDDFT calculations in MeOH on Gaussian 09 using the B3LYP functional and the 6-31G(d,p) basis set. The ECD spectra were generated using the SpecDis program and weighted according to the Boltzmann distribution after UV correction.

Cytotoxicity Asssay

Cell viability was assessed by CCK-8 method. The HepG2 cells were seeded into 96 well plate at density of 8×10^3/well, and cultured in MEM medium, supplemented with 10% fetal bovine serum (FBS) at 37 under 5% CO_2 in a humidified atmosphere. Then the cells were exposed to PA (1, 10, 100, 200, 250, 350 μ M) and compounds **1** –**18** (50 μ M). Twenty-four hours later, CCK-8 was added to test the cell viability. The absorbance was measured at 450 nm with a 96-well multilabel plate reader (PerkinElmer Life Sciences, Inc., Boston, MA, USA). The cell viability in the control group (cells were not treated by test samples and PA) was set as 100%.

Glucose Consumption Assay

HepG2 cells were exposed to PA (200 μ M) with the presence of 100 nM insulin to establish IR model in the following experiment. In the glucose consumption assay, the cells were seeded into 96 well plates with a density of 8×10^3 cells/well. The medium was replaced by MEM basic medium for starvation treatment with 6 h. HepG2 cells were cope with PA (200 μ M) for 24 h, and then the tested compounds at concentrations of 1.5625-50.0 μ M were added with serum-free medium containing 100 nM insulin. After additional 24 h, the

concentrations of glucose in supernatant were determined by Glucose Assay Kit following the manufacturer's instruction. Glucose consumption = glucose concentration of control group - glucose concentration of drug-treatment group.

ELISA Assay

The level of IL-1β in the culture supernatant were quantified using the corresponding ELISA kits (Solarbio Technology Co., Ltd., Beijing, China) following the manufacturer's instructions.

Evaluation of ROS

The expression levels of ROS were measured using the probe of 2',7'-dichloro-fluorescein diacetate (DCFH-DA). In brief, HepG2 cells were seeded into 6-well plates at 4×10^5 cells/well, and the intervention was performed according to the method outlined in Section 2.6. Then, the cells were incubated with 10 mM DCFH-DA for 30 min at 37°C in the dark. After incubation, cells were washed three times and harvested in free-serum medium. The fluorescences were then determined by a fluorescence microplate reader (500 nm excitation and 530 nm emission filters; Tecan Spark, Shanghai, China).

Western Blot Analysis

HepG2 cells were incubated with compound **9** and then stimulated with PA (200 μ M) for indicated time. Then, cells were washed, harvested, and coped with 1% RIPA lysis buffer to extract the total proteins. Cellular lysates were centrifuged (12 000 g for 10 min) and the supernatants were collected. Then the concentrations of the proteins were measured by the enhanced BCA Protein Assay Kit (Solarbio Technology Co., Ltd., Beijing, China) following to the manufacturer's procedure. Equal amounts of protein (30 μg/lane) were electrophoresed by sodium dodecyl sulfate polyacrylamide gel electrophoresis (SDS-PAGE, BioRad Laboratories, Hercules, CA) and transferred to polyvinylidene fluoride (PVDF) membranes (Bio-Rad Laboratories, Hercules, USA). The membranes were incubated with a 1:1000 dilution of primary antibodies overnight at 4 °C after blocking with 5% skim milk in TBST. Then membranes were washed twice with TBST buffer, and incubated with secondary antibodies for 2 h. Bound immuno-complexes were visualized by GE AI600 (GE Healthcare Life Science, Pittsburgh, America).

Supporting Information

The supporting information for this article is available on the WWW under https://doi.org/10.1002/cjoc.2021xxxxx.

Acknowledgement

This research work was financially supported from the National Natural Science Foundation of China (82003606), Scientific and Technological Key Project in Henan Province (212102311093), and Scientific Research Nursery Project (MP2020-29).

References

Li, D.; Wang, K.W. Natural new sesquiterpenes: Structural Diversity and Bioactivity. *Curr. Org. Chem.* **2016**, *20*, 994–10
(The following will be filled in by the editorial staff)
Manuscript received: XXXX, 2022 Manuscript revised: XXXX, 2022 Manuscript accepted: XXXX, 2022 Accepted manuscr

The Authors	The Authors After acceptance, please insert a group photo of the authors taken recently. **Left to Right:** Authors Names	The Authors

Entry for the Table of Contents

Posted on 28 Dec 2022 — The copyright holder is the author/funder. All rights reserved. No reuse without permission. — https://doi.org/10.22541/au.167226828.88800119/v1 — This a preprint and has not been peer reviewed. Data may be preliminary.

2,3/1,10-seco, 3-nor guaianolide-type sesquiterpenoids and their derivatives with hypoglycemic activity fron
Text for Table of Contents.

Posted on 28 Dec 2022 — The copyright holder is the author/funder. All rights reserved. No reuse without permission. — https://doi.org/10.22541/au.167226828.88800119/v1 — This a preprint and has not been peer reviewed. Data may be preliminary.